Cement & Concrete Composites 36 (2013) 42–47

Contents lists available at SciVerse ScienceDirect

Cement & Concrete Composites

journal homepage: www.elsevier.com/locate/cemconcomp

Measuring interparticle forces: Evaluation of superplasticizers for microsilica via colloidal probe technique

C. Glotzbach [a,*], D. Stephan [b], M. Schmidt [a]

[a] Department of Structural Materials and Construction Chemistry, University of Kassel, Mönchebergstr. 7, 34125 Kassel, Germany
[b] Department of Civil Engineering, Building Materials and Construction Chemistry, Technische Universität Berlin, Gustav-Meyer-Allee 25, 13355 Berlin, Germany

ARTICLE INFO

Article history:
Received 31 January 2012
Received in revised form 20 November 2012
Accepted 22 November 2012
Available online 1 December 2012

Keywords:
Aggregation
Silica fume
Surfactant
Rheology
Atomic force microscopy
Adhesion

ABSTRACT

Recent concretes like ultra-high performance concrete (UHPC) are comprised of large quantities of fines following a well-defined gradation to fill the voids between coarser particles, such as cement grains. The filling of voids displaces water, which positively influences the flowability. As the rheological properties of these fresh concretes depend mainly on the forces acting between the fines due to their high specific surface areas, understanding of these forces has become crucial. In this study, the atomic force microscopy technique of colloidal probes has been used to study the adhesive forces acting between individual silica particles placed in superplasticizer and electrolyte solutions, as silica exhibit the largest fraction of inner surface in common UHPC mixtures. Pairs of individual amorphous glass particles were approached and retracted from each other. Using this technique and silica particles as a model system, several commercial superplasticizers could be evaluated regarding their influence on the interparticle adhesion.

1. Introduction

The rheological properties of highly concentrated suspensions are governed by the direct interaction of their particles. Under given boundary conditions, increased attractive forces between the particles lead to a higher viscosity and hinder the flowability of the paste. Regarding ultra-high performance concrete (UHPC), many of its raw materials have been characterized and the influence of their properties on flowability has been studied. As UHPC is very rich in fine materials, these forces that act between the particle surfaces play a major role. Especially UHPC has a gradation of fines that is optimized for maximization of particle packing [1]. Its workability is adjusted without the addition of water only by the use of superplasticizers. This has been covered in more detail by Geisenhanslüke [2]. While the effects of interparticle forces on concrete are usually visualized macroscopically by spread value and flowability, it is necessary to find more direct means to measure the acting forces in order to understand the basic mechanisms for superplasticizers involved in the flow of cementitious pastes.

Atomic force microscopy (AFM) has now been used for two decades to study the forces between surfaces. Crystalline silicon dioxide surfaces belong to the most widely studied AFM samples as they behave inertly in a wide variety of conditions and as such permit easy handling of the samples. On the other hand, silica surfaces exhibit the largest surface in UHPC mortars. As can be seen in Table 1 [3], especially silica fume, while only constituting about 6 wt.% of all the solid materials in the mortar, is responsible for about 85% of the surface of the solids. The interactions of these fines dominate the rheological behavior of the mortar at large. For this reason, we have focused our research on silica surfaces.

In our experiments, we have approached two spherical particles in a closed cell flooded with different additive solutions. The forces acting between the particles were measured in a fluid environment that could be adapted to simulate a real mortar.

The flow behavior of suspensions like concrete depends mainly on the forces that act between individual particles (e.g. [4–6]). A wide range of superplasticizers have been used in the recent decades which help disperse the particles by overcoming adhesive forces, and ease tangential movement of the particles by hindering contact between them [7]. Understanding how these polymers adsorb onto different material surfaces and change the adhesive forces is therefore important. It is understood that modern polycarboxylate esters mainly act via steric repulsion. Though limited to silica surfaces for the time being, our method allows analyzing these forces directly over a wide range of experimental conditions.

2. Experimental study

2.1. Materials

For the force measurements, the surfaces that are to be studied have to be of known geometry, asperities must be only minimal.

* Corresponding author. Tel.: +49 561 804 3967; fax: +49 561 804 2662.
E-mail address: glotzbach@uni-kassel.de (C. Glotzbach).

0958-9465/$ - see front matter © 2012 Elsevier Ltd. All rights reserved.
http://dx.doi.org/10.1016/j.cemconcomp.2012.11.007

Table 1
Typical composition of ultra-high performance concrete [1].

Mass fraction (%)		Mass fraction (kg/m^3)	Surface area (m^2/m^3)	Surface fraction (%)
Fine sand 0/0.5	45.4	975	–	–
Cement 52,5-R HS/NA	38.7	832	386,880	12.2
Quartz powder	9.6	207	86,319	2.7
Silica fume	6.3	135	2700,000	85.1

– = value below measurement threshold.

Table 2
Chemical Composition of the glass beads acc to supplier.

Component (oxide)	Wt.%
SiO_2	72.50
Na_2O	13.00
CaO	9.06
MgO	4.22
Al_2O_3	0.58

Also, the particles have to be easy to handle for sample preparation. Therefore, glass beads (*SiLi 5210 S*, *Sigmund Lindner GmbH*, chemical composition see Table 2) with a typical diameter of 10 μm were used as a sample system for silica fume as depicted in Fig. 1: For each measurement, one bead was fixed onto a glass substrate, another bead was fixed onto the tip of a tipless cantilever (*Mikromasch CSC-12 tipless/NoA*, typical spring constant k = 0.1 N/m) by means of a two-component methacrylate epoxy resin (*Uhu plus endfest 300*). All beads were subject to ultrasonic treatment to separate glass splinters from their surfaces. Before the tests, the smoothness of the surfaces was validated by measuring their topography over an area of 5 × 5 μm^2 via contact mode AFM. After fitting the surfaces to a second order polynom to accommodate the surface curvature of the beads, the roughness was quantified as the root mean square of the height over the base plane (see Fig. 2 as an example). All used beads had an *rms* roughness (root mean square) of up to 6 nm (Ref. Table 3). Beads with higher roughness or large asperities were rejected. The radius of the beads was measured by SEM imaging.

Four polymers were used in this study: a commercially available PCE superplasticizer ("PV", M_w = 81,000 Da), a custom-synthesized polymer [8] ("CS", methacrylic acid and (ω-methoxypolyethylene glycol)-methacrylate with methallyl sulfonic acid as a chain transfer agent, M_w = 29,200 Da, side chains 12 nm, backbone 13 nm), a melamine sulfonat ("MS"), and polyacrylate acid ("PAA") for comparison.

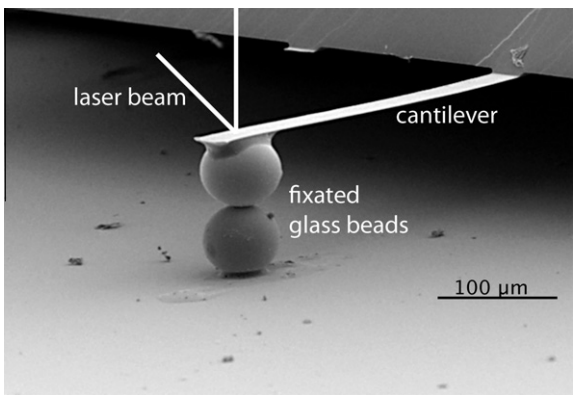

Fig. 1. SEM model of the AFM test setup with glass beads of about 70 μm, larger than those used in the study. The laser path is shown for illustration purposes.

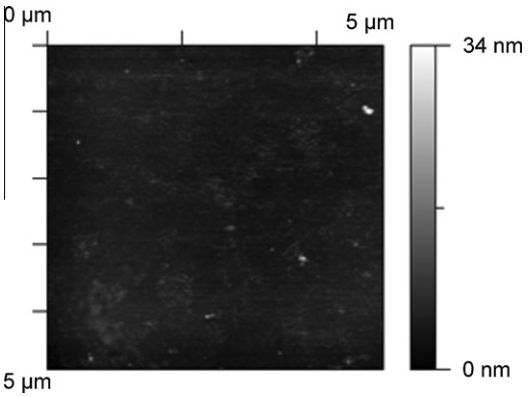

Fig. 2. AFM image of a bead surface after fitting the curvature of the sphere to a polynom of 2nd order.

Table 3
The bead combinations used for the polymers, and their characteristics.

Additive	Cantilever spring constant (N/m)	Cant. bead size (μm)	Bottom bead size (μm)	Reduced radius (μm)
CS	0.14	13.1 (*rms* = 4.5 nm)	15.3 (*rms* = 2.2 nm)	7.06
PV	0.12	12.2 (*rms* = 5.8 nm)	14.2 (*rms* = 3.4 nm)	6.56
MS	0.15	16.8 (*rms* = 5.0 nm)	13.1 (*rms* = 3.7 nm)	7.36
PAA	0.14	14.4 (*rms* = 6.0 nm)	14.2 (*rms* = 5.7 nm)	7.15

rms values are the root mean square of surface height and indicate surface roughness.

The test solutions were prepared with water purified by reversed osmosis and CDI (*VWR GPR Rectapur*). Polymer solutions as provided by the manufacturer were diluted to mass concentrations of 1%, 0.1%, 0.01%, 0.001%, and 0.0001%, thus taking into account that only a small fraction of the polymer molecules in a mortar may be available for a given pair of particles.

2.2. Testing procedures

2.2.1. Determination of cantilever spring constants

The spring constants were determined by the Cleveland method [9] and additionally taking further origins of errors into account. For this, the resonance frequency of the cantilevers was measured before and after modifying them with a bead, yielding the spring constant k. The inclination of the cantilever was measured at 12°; the spring constant was therefore corrected by the factor $\cos^{-2}\alpha$ as proposed by the manufacturer of the microscope. Also, resulting spring constant after Cleveland would only be valid if the center of the bead were just beneath the outer end of the cantilever. As this could not be achieved, the distance ΔL by which the bead was off the end position of the cantilever (Fig. 3) was used to correct the spring constant by terms, derived [10] from a method described by Gibson [11]: For this, the oscillating cantilever is thought to be a pendulum with an oscillation frequency of $\nu \sim J^{-1/2}$, J being its inertial moment.

In their theoretical model, Cleveland et al. [9] view the combined masses of cantilever and attached particle as a mass attached to spring. But it can be assumed instead that the oscillating cantilever of length L is an effective mass m^* that is concentrated in one point, and is rotating at a distance of L around the fixed bearing

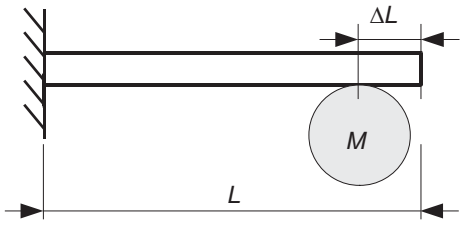

Fig. 3. Off-end loading: the bead is displaced by ΔL from the end of the cantilever of length L.

(like a pendulum). If a bead with a weight M is added that is equally a point mass fixed to the cantilever at a distance of $L - \Delta L$ from the bearing, the inertial moment J' of the combined system is calculated as:

$$J' = m^* \cdot L^2 + M(L - \Delta L)^2 \quad (1)$$

while if the bead were fixed exactly at the end of the cantilever, the inertial moment J of the system would be just

$$J = (m^* + M)^2 \cdot L \quad (2)$$

The measured resonance frequency of the oscillating cantilever according to Cleveland with a bead fixed with a displacement of ΔL from the outermost end of the cantilever therefore has to be corrected by the factor $J'^{-1/2}/J^{-1/2}$, yielding the corrected oscillation frequency ν_{corr} that can be used in Cleveland's formula.

$$\nu_{corr} = \frac{\sqrt{m^* \cdot L^2 + M(L - \Delta L)^2}}{\sqrt{(m^* + M)^2 \cdot L}} \quad (3)$$

The displacement ΔL of the loaded bead from the end of the cantilever is measured via SEM. But even then, the cantilever constant k calculated via Cleveland is only valid for the outer-most end point of the cantilever, while the length at which the cantilever operates on the sample is dependent on the off-end loading ΔL. Therefore, a correction factor proposed by Sader et al. [12] is used:

$$k_{corr} = k \cdot \frac{L^3}{(L - \Delta L)^3} \quad (4)$$

The resulting cantilever constant k_{corr} is used for the calculations.

2.2.2. Force measurement

A glass substrate with a bead fixed onto it was inserted into the sample holder of the atomic force microscope (*Veeco MultiMode, Nanoscope IV*); a cantilever with another bead was put into the chip holder of the fluid cell. Both beads were placed atop each other (see Fig. 1), but were kept at distance at first. The fluid cell was sealed off with an o-ring. Then the test fluids were drawn into the cell using a syringe through tubing. This was repeated until no air bubbles were left in the fluid cell. The tubing was then removed from the fluid cell and replaced with two caps to prevent CO_2 from the air diffusing into the test solution. The system was left for 5 min to reach adsorption equilibrium. Afterwards, the beads were brought into contact at their outermost points, meaning that both centers as well as the contact point between them were in one straight line. Around this position, a matrix of 10 by 10 matrix points was defined in an area of $50 \times 50\ nm^2$, resulting in a series of 100 measurements for one test solution. After moving the bottom bead to each of these matrix positions, the force was measured by pushing the beads together with a defined force of 42 nN and pulling them apart again. The measurement frequency was 0.5 Hz. This was repeated for all solutions of one polymer, starting with the lowest concentrations. Each pair of top bead and bottom bead was used for one polymer series only.

2.2.3. Shear resistance

The torque was measured for particle suspensions (mass ratio DI water/beads 1:3.5) in a rotational coaxial rheometer (*Schleibinger Viskomat NT*) with constant rotation with 120 rpm. The salts were added in several steps. Before each further addition, a steady state was observed for the torque values. The shear resistance was measured as the torque exerted by the rotating suspension on a steady paddle.

3. Results and discussion

During the force measurements, the deflection of the cantilever was measured while the distance between the particles was gradually changed. While the beads were apart from each other, the cantilever deflection was zero as no force was acting on the bead. The cantilever base was moved down along the z axis by piezo actuators. As soon as the beads contacted each other and were pushed together with a force of 42 nN, the cantilever was deflected. Then the cantilever was pulled away again. The two beads were then in contact and would not separate, deflecting the cantilever in the opposite direction. The cantilever was pulling the top bead away from the fixed bottom bead. Only if the pulling force exacted from the deflected cantilever was at least as large as the adhesive force between the beads, they could be separated again. This leads to a theoretical measurement cycle as depicted in Fig. 4.

The adhesive force F between the beads is then calculated as the maximum deflection x multiplied by the effective spring constant keff.

F depends on the size of the conjoint areas of the beads. When the radii of the particles increase, the resulting contact area

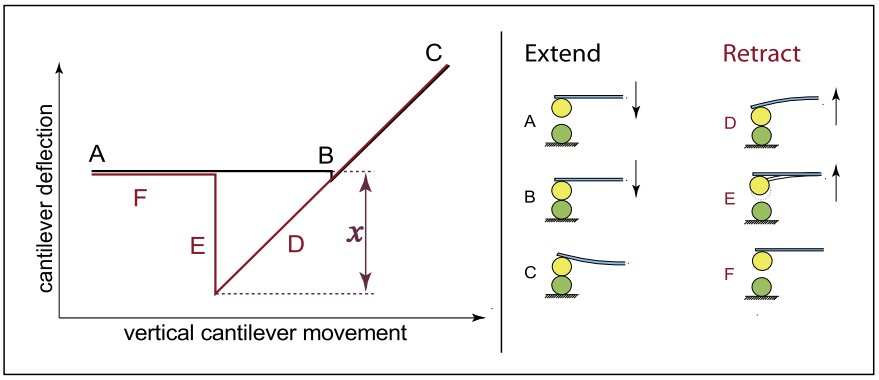

Fig. 4. One optimal single force measurement cycle.

between the two beads gets larger. As not all beads are of the same size, all resulting adhesive forces were normalized by division by the reduced radius

$$R' = \frac{R_1 R_2}{R_1 + R_2} \tag{5}$$

as described by Butt et al. [13], taking both individual bead radii R_1 and R_2 into account and yielding the normalized adhesive force F'.

$$F' = \frac{F}{R'} \tag{6}$$

While evaluating the adhesive forces worked fine for saline solutions, polymer solutions could not be measured as there was often no single point of failure in the adhesion of the beads, but rather a gradual failure where the beads separated slowly away from each other. This was interpreted as the beads being held together by the chains of the polymers, only gradually desorbing from the silica surfaces. Thus, for evaluating the adhesion when polymer molecules were present in the solution, the force pulling the beads apart was integrated over the course of the separation of the beads:

$$E_A = \int_{z_e}^{z_i} F' dz \tag{7}$$

where z_i is the initial z position of the moving cantilever base at the beginning and also the end of the cycle (position F in Fig. 4), and z_e is the z position when both beads are in contact, but no force is exacted on them by the cantilever (position B in Fig. 4). dz is an infinitesimal movement of the cantilever base along the z axis. This yields the adhesion energy E_A that has to be overcome to separate the two beads as the normalized forces F' have been integrated over the distance traveled by the cantilever. E_A is additionally normalized by the reduced radius R'. Therefore E_A is measured in (nN nm)/μm = pJ/m.

The indicated values are averaged over all 100 measurements for one sample and test solution.

3.1. Comparison of predictions and experimental results

Measuring the adhesive force between two beads in deionized water resulted in a normalized force of 11 nN/μm. Using the equation from [14]:

$$A_H = -\frac{F}{R'} \times 12D^2 \tag{8}$$

to calculate the Hamaker constant A_H for two silica particles in contact (distance between particles D = 0.2 nm when the particles are in direct contact) yields $A_H = 5.3 \times 10^{-21} J$, which is in accordance with the range of values for two silica surfaces in water in literature [14,15]. This indicates that the resulting forces measured by this method are valid.

3.2. Correlation between adhesive force and rheological behavior

To show the effect of the adhesive force on the macroscopical rheological flow behavior of a suspension, the adhesive forces between two particles were measured in electrolyte solutions of NaCl and $CaCl_2$. It is correlated with the change in shear resistance during successive addition of the same salts during the measurement in a rheometer, shown in Fig. 5. The divalent Ca^{2+} ions shield the surface charge of the silica surface much stronger than the monovalent Na^+ ions. At the same electrolyte concentration at which a steep rise in adhesive force could be measured (about 0.01 mol/L) and the shear resistance of the suspension showed a similarly steep increase. Na^+ on the other side led to a smaller rise in adhesion and therefore a weaker shear resistance.

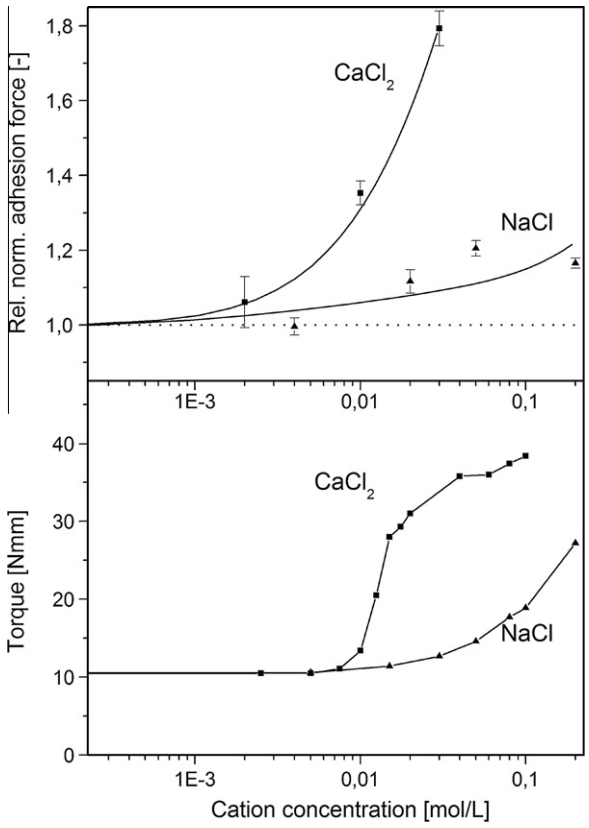

Fig. 5. Correlation of the increasing adhesive force between two individual and the equally increasing shear resistance of a suspension in relation to a different electrolyte concentrations (NaCl and $CaCl_2$). The adhesive force is given as ratio to the adhesive force in deionized water.

3.3. Experimental results and discussion

Though the adhesion forces showed the same tendency as the calculated adhesion energies, we evaluated the adhesion energies only, because the gradual failure of the adhesive bond between two beads did not show one single pull-off, but sometimes several. The normalized adhesion energy thus offers more substantial data.

The calculated adhesion energies that were normalized by the reduced radius of the used bead combinations show similar values for all used combinations when they were submerged in equal liquid environments, i.e. in pure water. This indicates that the results for all used bead combinations are comparable, and that the screening of beads was appropriate and also successful.

The normalized adhesion energies differ significantly between the studied polymers (see Fig. 6). The rather large polymers PV did not reduce the energy necessary to separate the beads for a concentration of 10^{-4} wt.%. The values rather show a slight increase in adhesion energy. But this small rise is not significant and can as well be attributed to statistical spread. Only after reaching a concentration of 0.1 wt.% is the adhesion energy reduced to a level that was reached with much lower concentrations for the other polymers.

Polymer PV is a commercially available additive for concrete fluidization. It is rather large ($M_w \approx 80.000$ kDa) with long side chains in comparison with CS and its shorter side chains. The main difference between CS and PV is in architecture of the molecules. The latter shows a significant reduction in adhesion energy already at the lowest tested concentration, i.e. 10^{-4} wt.%. Increasing the concentration does not lead to a further decrease in adhesion energy.

PAA and MS show a similar behavior like CS, i.e. a strong decrease in adhesion at low concentrations. PAA generally show higher adhe-

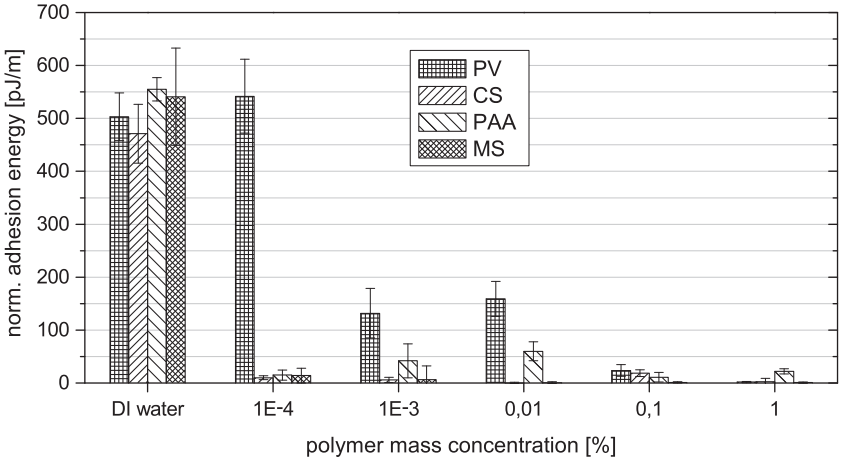

Fig. 6. Normalized adhesion energy between two beads for four polymers in increasing concentration.

sion. This polymer is in principle just the backbone of a superplasticizer with no ester groups as side chains. Therefore, there is only one functional group that can adsorb on a bead's surface, and this group is equally distributed along the whole chain of the polymer. When two beads are in contact, there are many polymer molecules that are in contact with both beads and can therefore bridge them, leading to a more pronounced bond between them.

The large molecules of PV on the other hand have a long backbone together with long side chains. One would assume this to lead to a strong steric repulsion. But as can be seen in Fig. 6, these molecules do not disperse the silica beads as well as the others. In fact, there is still a pronounced adhesion energy that has to be overcome to separate the particles. This might be due to the protruding side chains strongly adsorbing to the surface of the adjacent bead, and thus bridging the particles and holding them together. The typical PEO sequences in the side chains are known to have a high affinity to silica surfaces [16]. Furthermore, even the long backbone of the polymer might be able to bridge the particles. The results for PAA, which essentially is the backbone of PV, show indeed slightly higher adhesion energy than CS which could support this. The higher level of adhesion energies for PV can also be attributed to the tangling of the side chains of polymers adsorbed to adjacent particles.

While shearing a suspension, many particles come into contact with each other throughout the suspension and have to be separated again for the motion to continue. If they are strongly bound to each other, this will hinder the suspension flow. This would mean that strong adhesion energies will lead to a poorer workability. From the presented results, one can easily deduce that PV is not the perfect plasticizing agent for silica surfaces, e.g. silica fumes.

In concretes though, there are many chemically different surfaces that have to be dispersed, where these molecules might again prove more efficient. For the studied combination of two silica particles, PV seems the least efficient while CS and MS are more effective.

4. Conclusions

Atomic force microscopy can be used to measure the forces not only between specialized and custom made cantilever tips as they are common in the AFM community. Rather, whole particles can be measured, though some obstacles have to be overcome. Well defined surfaces are of utmost importance to the success of the measurements. Even the relatively smooth particles used in this study led to a significant variance in adhesion energies that was larger for combinations of beads with larger roughness. This results in reduced resolution for measured adhesive energies. The distribution of adhesion energies for one bead pair was broader when the particles showed a higher *rms* roughness. These have to differ significantly between two polymers if they are to be compared.

Adhesion energies describe the whole process of two contacted particles being completely separated again from each other. Gradual desorption of polymers is taken into account by integrating over all the adhesive forces along the movement of the cantilever until they separate again.

Large polymers may bridge the gap between two particles and bind them together if their constituents have a high affinity to the neighboring bead surfaces. The technique can specifically help identify more closely the reason of what is usually only considered an incompatibility of plasticizers and particles. In this case, a bridging between particles can be observed.

Special attention was paid to fine-tuning the Cleveland method for determining the cantilever constant. It was refined to yield the effective cantilever constant relevant to the shown test setup, taking into account fixing the colloidal probe to the cantilever with a displacement from the outer edge. The displacement is typically not taken into account when the cantilevers are calibrated using the method from Sader et al. [12] The Cleveland method itself is very adequate for the used test setup as it essentially involves bead fixation to the cantilever, a procedure that is also required for the colloidal probe setup.

Acknowledgments

The presented study is part of a research project about UHPC generously supported by the DFG for which we are thankful. We would furthermore like to thank Wolfgang Peukert and Bettina Winzer from the University of Erlangen-Nürnberg, Germany, who helped us to set up the experiments. We also deeply appreciate the help and work of Sandra Schink who carried out part of the shown AFM measurements, and Christof Schröfl [8] who provided us with custom superplasticizer polymers.

References

[1] Reschke T. Der Einfluss der Granulometrie der Feinstoffe auf die Gefügeentwicklung und die Festigkeit von Beton. PhD thesis. Germany. Schriftenreihe der Zementindustrie: Bauhaus University Weimar; 2000.
[2] Geisenhanslüke C. Influence of the granulometry of fine particles on the rheology of pastes. PhD thesis, Univ. of Kassel, Structural materials and engineering series Kassel University Press, Kassel: Germany; 2009, 13.
[3] Stephan D, Krelaus R, Schmidt M. Direct measurement of particle–particle interactions of fines for UHPC using AFM technology. In: Proc 2nd int symp on ultra high performance concrete. Kassel University Press, Kassel, Germany, 2008, p. 375–381.3.

[4] Uchikawa H, Hanehara S, Sawaki D. The role of steric repulsive force in the dispersion of cement particles in fresh paste prepared with organic admixture. Cem Conc Res 1997;27:37–50.
[5] Yamada K, Hanehara S. Interaction mechanism of cement and superplasticizers – the role of polymer adsorption and ionic conditions of aqueous phase. Conc Sci Eng 2001;3:135–45.
[6] Yoshioka K, Sakai E, Daimon M, Kitahara A. Role of steric hindrance in the performance of superplasticizers for concrete. J Am Cer Soc 1997;80:2667–71.
[7] Napper DH. Steric Stabilization. J Coll Int Sci 1997;58:390–407.
[8] Schröfl C. omega-Methoxypoly(ethylenoxid)-Methacrylsäureester-co-Methacrylsäure-co-Methallylsulfonsäure-Polycarboxylate als Fließmittel für ultrahochfesten Beton: Synthese, Wirkmechanismus und Untersuchungen zum Synergismus von selektiv adsorbierenden Polymergemischen. PhD thesis, TU München; 2010.
[9] Cleveland JP, Manne S, Bocek D, Hansma PK. A nondestructive method for determining the spring constant of cantilevers for scanning force microscopy. Rev Sci Instrum 1993;64:403–5.
[10] Glotzbach C. Interpartikuläre Wechselwirkungen in wässrigen Medien an einem Modellsystem für Feinstoffe Diploma Thesis. Kassel: Kassel University; 2008.
[11] Gibson C, Smith D, Roberts C. Calibration of silicon atomic force microscope cantilevers. Nanotechnology 2005;16:234–8.
[12] Sader JE, Larson I, Mulvaney P, White LR. Method for the calibration of atomic force microscope cantilevers. Rev Sci Instr 1995;66:3789.
[13] Butt HJ, Cappella B, Kappl M. Force measurements with the atomic force microscope: technique, interpretation and applications. Surf Sci Rep 2005;59:1–152.
[14] Butt HJ, Graf K, Kappl M. Physics and chemistry of interfaces. Weinheim: Wiley-VCH; 2006.
[15] Lee I. Friction and adhesion of silica fibers in liquid media. J Mater Sci 1995;30:6019–22.
[16] Orgeret-Ravanat C, Gramain P, Déjardin P, Schmitt A. Adsorption/desorption of a PEO-rich comb-like polymer at a silica/aqueous solution interface. Coll Surf 1988;33:109.